

RESEARCH

Open Access



Distinguishing the effects of systemic CSF1R inhibition by PLX3397 on microglia and peripheral immune cells

Akhabue K. Okojie^{1,2*}, Joseph O. Uweru^{1,2}, Morgan A. Coburn^{1,2}, Sihan Li¹, Vivian D. Cao-Dao^{1,2} and Ukpong B. Eyo^{1,2*}

Abstract

Microglia, the primary immune cells of the central nervous system (CNS), are derived from the yolk sac and populate the brain during development. Once microglia migrate to the CNS, they are self-renewing and require CSF1R signaling for their maintenance. Pexidartinib (PLX3397, PLX), a small molecule inhibitor of the CSF1R, has been shown to effectively deplete microglia since microglial maintenance is CSF1R-dependent. There have, however, been several conflicting reports that have shown the potential off-target effects of PLX on peripheral immune cells particularly those of lymphoid origin. Given this controversy in the use of the PLX family of drugs, it has become important to ascertain to what extent PLX affects the peripheral immune profile in lymphoid (spleen, and bone marrow) and non-lymphoid (kidney, lungs, and heart) organs. PLX3397 chow treatment at 660 mg/kg for 7 days significantly reduced CD45⁺ macrophages, CX3CR1-GFP cells, CD11b⁺CD45^{intermediate} cells, and P2RY12 expression in the brain. However, there were minimal effects on peripheral immune cells from both lymphoid and non-lymphoid organs except in the heart where there was a significant decrease in CD3⁺ cells, inflammatory and patrolling monocytes, and CD11b⁺Ly6G⁺ neutrophils. We then stimulated the immune system with 1 mg/kg of LPS which resulted in a significant reduction in the number of innate immune cells. In this context, PLX did not alter the cytokine profile in the serum and the brain of naïve mice but did so in the LPS-stimulated group resulting in a significant reduction in TNF α , IL-1 α , IFN- γ and IL-1 β . Furthermore, PLX did not alter locomotor activity in the open field test suggesting that microglia do not contribute to LPS-induced sickness behavior. Our results provide an assessment of immune cell populations with PLX3397 treatment on brain, lymphoid and non-lymphoid organs without and during LPS treatment that can serve as a resource for understanding consequences of such approaches.

Keywords CSF1R inhibitor, PLX3397, Microglia, LPS, Cytokines, Sickness behavior, Peripheral immune cells

Background

Microglia are the primary immune cells of the central nervous system (CNS) and make up 5–10% of the cells in the CNS [40]. Once microglia migrate to the CNS during development, they become self-renewing and require colony-stimulating factor 1 receptor (CSF1R) signaling for their maintenance [17, 19, 27, 53, 73, 76]. CSF1 acting through CSF1R controls the differentiation of macrophages from monocytes when recruited into peripheral tissues. Pexidartinib (PLX3397), a small

*Correspondence:

Akhabue K. Okojie
gsg4pb@virginia.edu
Ukpong B. Eyo
ube9q@virginia.edu

¹ Department of Neuroscience, University of Virginia School of Medicine, Charlottesville, VA, USA

² Center for Brain Immunology and Glia, University of Virginia School of Medicine, Charlottesville, VA, USA



© The Author(s) 2023. **Open Access** This article is licensed under a Creative Commons Attribution 4.0 International License, which permits use, sharing, adaptation, distribution and reproduction in any medium or format, as long as you give appropriate credit to the original author(s) and the source, provide a link to the Creative Commons licence, and indicate if changes were made. The images or other third party material in this article are included in the article's Creative Commons licence, unless indicated otherwise in a credit line to the material. If material is not included in the article's Creative Commons licence and your intended use is not permitted by statutory regulation or exceeds the permitted use, you will need to obtain permission directly from the copyright holder. To view a copy of this licence, visit <http://creativecommons.org/licenses/by/4.0/>. The Creative Commons Public Domain Dedication waiver (<http://creativecommons.org/publicdomain/zero/1.0/>) applies to the data made available in this article, unless otherwise stated in a credit line to the data.

molecule inhibitor of CSF1R, has been shown to effectively deplete microglia in a dose and duration-dependent manner since microglia renewal and proliferation are CSF1R-dependent [8, 17, 24, 29, 33, 66]. PLX3397 is an oral tyrosine kinase inhibitor that is in phase 1–3 clinical trials for the treatment of different cancers [10]. PLX3397 has also been reported to interfere with other tyrosine kinases c-Kit and Fms-like tyrosine kinase 3 (FLT3) [67], which could have an impact on other immune cells. PLX3397 is also being tested for its potential in treating non-cancerous diseases such as rheumatoid arthritis and multiple sclerosis [52].

There have, however, been several reports of off-target effects of PLX on peripheral immune cells primarily those of the lymphoid origin [29, 43]. Thus, it has become important to ascertain to what extent PLX3397 affects the peripheral immune profile since we recently documented effects of PLX3397 at a high concentration of 660 mg/kg for 7 days on the vasculature [8] and seizures [24]. Here, we examined consequences to the peripheral immune profile in lymphoid (spleen, and bone marrow) and non-lymphoid organs (kidney, lung, and heart) as well as serum and brain cytokines, sickness behavior, and downstream cellular signaling kinases.

We report that PLX3397 did not alter the number of peripheral immune cells from both myeloid and lymphoid origin in lymphoid and non-lymphoid organs except in the heart where we observed a significant reduction in some immune cells. Furthermore, the treatment of mice with 1 mg/kg of LPS resulted in a significant reduction in the numbers of peripheral innate immune cells but LPS-induced sickness behavior was preserved with PLX3397 treatment suggesting a sufficiently intact sickness behavior response without microglia. Finally, PLX3397 did not alter cytokines nor cellular kinases in homeostatic conditions, however, following LPS stimulation, PLX3397 resulted in significant reductions in IFN- γ in serum and IL-1 α , IL-1 β , and TNF α in the brain. Our results, therefore, suggest that PLX3397 significantly depletes the microglia population in the brain but does not have a dramatic effect on the peripheral immune profile in both lymphoid and non-lymphoid organs (except for innate immune cells following LPS treatment) nor

the serum and brain cytokines, and downstream cellular signaling kinases during Gram-negative bacterial infection.

PLX3397 eliminates microglia in the mouse brain

The extent of microglia depletion in the mouse brain was determined using flow cytometry and immunohistochemistry (IHC). We found that mice placed on PLX3397 (660 mg/kg) for 7 days (Fig. 1a) had a significantly reduced number of CD45⁺ macrophages and CX3CR1^{GFP/+} cells in the brain (Fig. 1b, c). We also found that CD11b⁺CD45^{intermediate} (microglia) cells were significantly reduced in the brain compared to mice fed control chow (Fig. 1d, e). The significant reduction in microglial number was also associated with a significant reduction in P2RY12 (a microglial-specific marker) expression in the PLX3397 fed group (Fig. 1f). In addition, IHC for CX3CR1^{GFP/+} showed that microglia were significantly reduced in the cortex and hippocampus compared to mice fed control chow (Fig. 1g–j) resulting in 86.8% and 73.5% decrease in microglia/field of view (FOV) following 7 days of PLX3397 diet in the cortex and hippocampus, respectively. This represents a ~80.2% decrease in microglia in the brain by IHC. Taken together, our data show that 7 days of PLX3397 (660 mg/kg) in chow significantly reduced CD45⁺ macrophages, microglial density, and P2RY12 expression in mice indicating an effective depletion of tissue-resident macrophages in the CNS.

PLX3397 does not affect immune cell numbers in lymphoid organs (bone marrow and spleen)

Having confirmed an effective depletion of brain-resident macrophages (microglia) by PLX3397, we sought to interrogate its effects on immune cell numbers in the periphery during the same period. We began by examining prime lymphoid organs. The bone marrow is one of the main lymphoid organs where immature lymphocytes differentiate to mature ones and subsequently migrate to a secondary lymphoid organ like the spleen. Several conflicting data have reported that CSF1R inhibitors impact peripheral immune cell numbers including classical inflammatory monocytes (CD11b⁺Ly6C^{hi}) or the non-classical inflammatory monocytes (CD11b⁺Ly6C^{low}) [29,

(See figure on next page.)

Fig. 1 PLX3397 eliminates microglia in the mouse brain. **a** Diagram of experimental illustration of mice placed on PLX3397 for 7 days followed by flow cytometric and immunohistochemistry for microglial density. **b** Representative image showing gating strategy and dot plot of CD45^{inter}CD11b⁺. **c** Quantification of CD45⁺ macrophage from single cell population from the brain. **d** Quantification of CX3CR1-GFP⁺ population following PLX3397 chow for seven days. **e** Quantification of the percentage of CD45^{inter}CD11b⁺ (microglia) population from CD45⁺ cell. **f** Quantification of P2RY12 expression from CD45^{inter}CD11b⁺ population. Representative images of the cortex (**g**) and the hippocampus (**h**) showing microglia after seven days of PLX3397 in chow. **i, j** Quantification of microglial density from the cortex (**i**) and the hippocampus (**j**) per field of view. Data were analyzed with unpaired Student's *T*-test, $n = 4-6$, and data represented by mean \pm SEM, *** $p < 0.001$, **** $p < 0.0001$

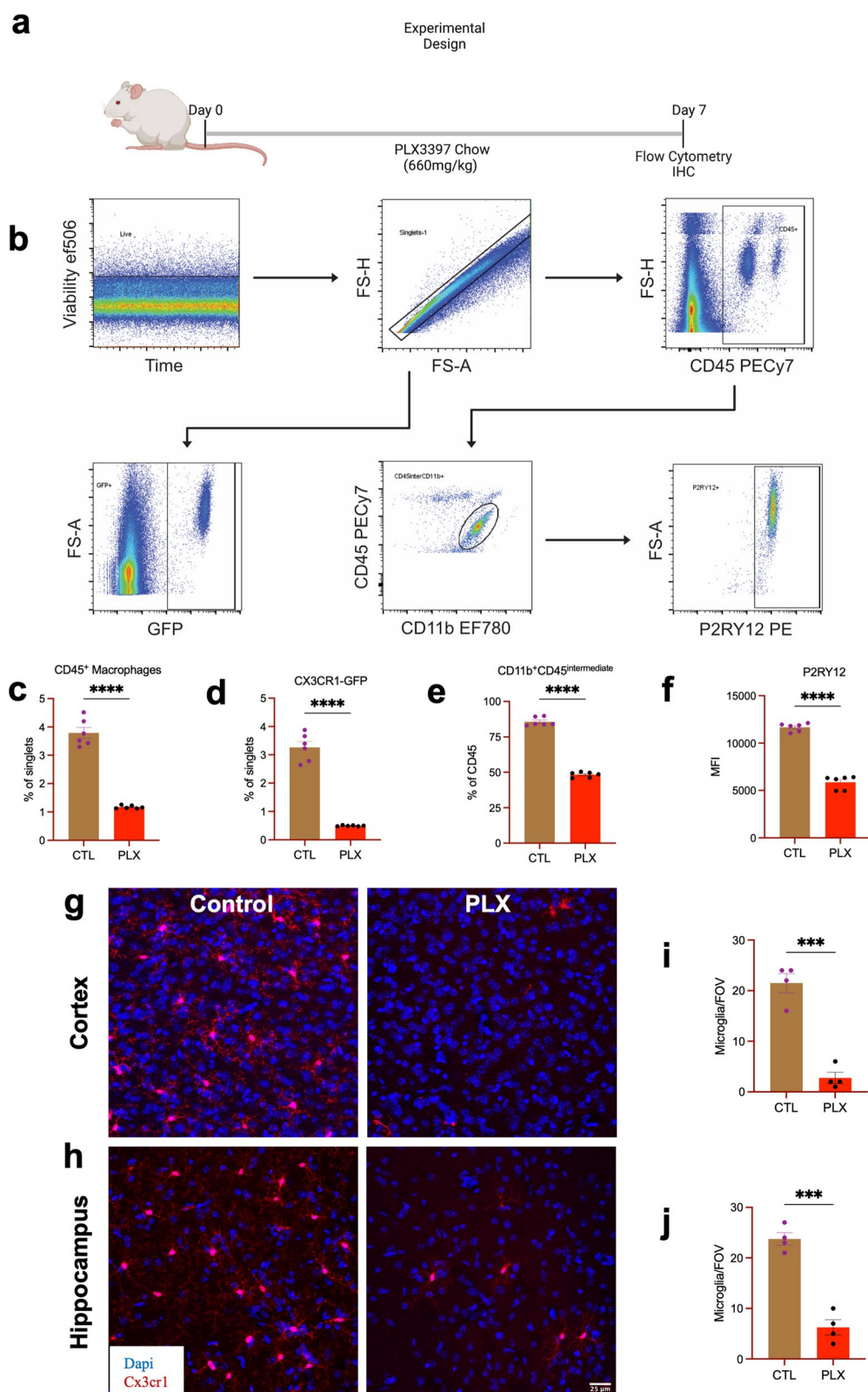


Fig. 1 (See legend on previous page.)

33, 43, 49, 66, 78]. To determine whether a high dose of PLX3397 impacts peripheral myeloid and lymphoid cell numbers in the homeostatic state, we quantified different populations of immune cells in the bone marrow and spleen in mice fed a high dose of PLX3397 for 7 days. We employed the gating strategy shown in Additional file 1: Fig. S1 in determining the various cell populations except in non-lymphoid organs where we had to first gate on CD45 from the size gate. We found that PLX3397 had no effect on the numbers of myeloid and lymphoid cells in the bone marrow and spleen (Fig. 2a–q). However, we found a marginal but significant depletion of Ly6C^{low} monocytes in the spleen of PLX3397-fed mice (Fig. 2r). Our data suggest that a high dose of PLX3397 for 7 days does not have a dramatic effect on peripheral immune cell numbers in the bone marrow and spleen.

Immune cell numbers in non-lymphoid organs (lungs and kidneys) are not altered by PLX3397

We next evaluated effects of PLX on non-lymphoid organs including the lungs and kidney. We observed that there was no significant effect on the myeloid and lymphoid cell populations in both the lung and kidney (Fig. 3a–r) indicating that a high dose of PLX3397 for 7 days does not negatively impact peripheral immune cell numbers in the lungs and/or kidneys.

PLX3397 has a minor effect on immune cell numbers in the heart

In addition to the kidney and lung, we also examined the heart as a non-lymphoid organ. Contrary to results obtained for the lung and kidney, we observed that a high dose of PLX3397 for 7 days resulted in a significant decrease in CD3⁺ (Fig. 4a), NK1.1⁺ (Fig. 4d), CD11b⁺Ly6G⁺ (Fig. 4f), Ly6C^{hi}, and Ly6C^{low} (Fig. 4g, h) cells compared to control. However, there was no significant difference between PLX3397 and the control chow-fed group with CD4⁺, CD8a⁺, CD19⁺, and MHC II⁺ cells (Fig. 4b, c, e, i). Taken together, these data show that PLX3397 causes a reduction in some peripheral immune cell populations in the heart.

Innate immune cell numbers are negatively impacted by PLX3397 in lymphoid and non-lymphoid organs after LPS treatment

Next, we attempted to determine the impact of PLX3397 on immune cell numbers during a Gram-negative bacterial infection. Lipopolysaccharide (LPS), which is a component of the Gram-negative bacteria, is a commonly used endotoxin that serves as a murine model to induce systemic and neuroinflammation and mimic Gram-negative bacterial infection. To determine to what extent PLX3397 impacts immune cell numbers from both myeloid and lymphoid compartments using the spleen (lymphoid organ) and lung (non-lymphoid organ), we stimulated the immune system with 1 mg/kg of LPS on the 7th day of a high PLX3397 diet then performed flow cytometry evaluation. Our results show that there was no significant effect on the number of adaptive immune cells (CD3⁺, CD4⁺, CD8⁺, NK1.1⁺, and CD19⁺) and MHCII⁺ cells in both the spleen and lung at 6 h. However, we observed a significant decrease in innate immune cell numbers including CD45⁺CD11b⁺Ly6C^{hi} (inflammatory) monocytes, CD45⁺CD11b⁺Ly6C^{low} (patrolling) monocytes, and CD11b⁺Ly6G⁺ neutrophils in the PLX-fed group compared to the control group in both the spleen and the lung (Fig. 5a–r). Taken together, PLX3397 treatment yields a significant decrease in cells involved in the innate immune system following LPS stimulation.

PLX3397 alters inflammatory cytokine levels (but not cellular kinases) in the serum and brain following LPS treatment

Following the observation that LPS treatment results in a decrease in innate immune cell numbers, we decided to ascertain to what extent PLX impacts cytokine secretion following endotoxin stimulation using 1 mg/kg of LPS. Following this treatment, we performed a Luminex assay assessment after 6 h on serum (Fig. 6a). Our results show that in the basal state, there was no significant difference between control and PLX3397-fed mice in all the serum cytokines profiled except for IL-13 which was significantly reduced in the PLX3397-fed group compared to control (Fig. 6b). However, stimulation with LPS resulted in a significant decrease in M-CSF, IFN γ , and CXCL10 in the PLX3397-fed group, while there was a significant increase in CCL3 in the control group

(See figure on next page.)

Fig. 2 PLX3397 does not affect immune cell numbers in lymphoid and non-lymphoid organs (bone marrow and spleen). Bar graphs show the number of immune cells from the bone marrow: **a** CD3⁺, **b** CD4⁺, **c** CD8a⁺, **d** NK1.1⁺, **e** CD19⁺, **f** CD11b⁺Ly6G⁺, **g** MHCII⁺, **h** CD11b⁺Ly6C_{low} (patrolling monocytes), **i** CD11b⁺Ly6C^{high} (inflammatory monocytes); and the spleen: **j** CD3⁺, **k** CD4⁺, **l** CD8a⁺, **m** NK1.1⁺, **n** CD19⁺, **o** CD11b⁺Ly6G⁺, **p** MHCII⁺, **q** CD11b⁺Ly6C_{low} (patrolling monocytes), **r** CD11b⁺Ly6C^{high} (inflammatory monocytes). Data were analyzed with unpaired Student's T-test, n = 3–6, and data represented by mean \pm SEM, **p* < 0.05

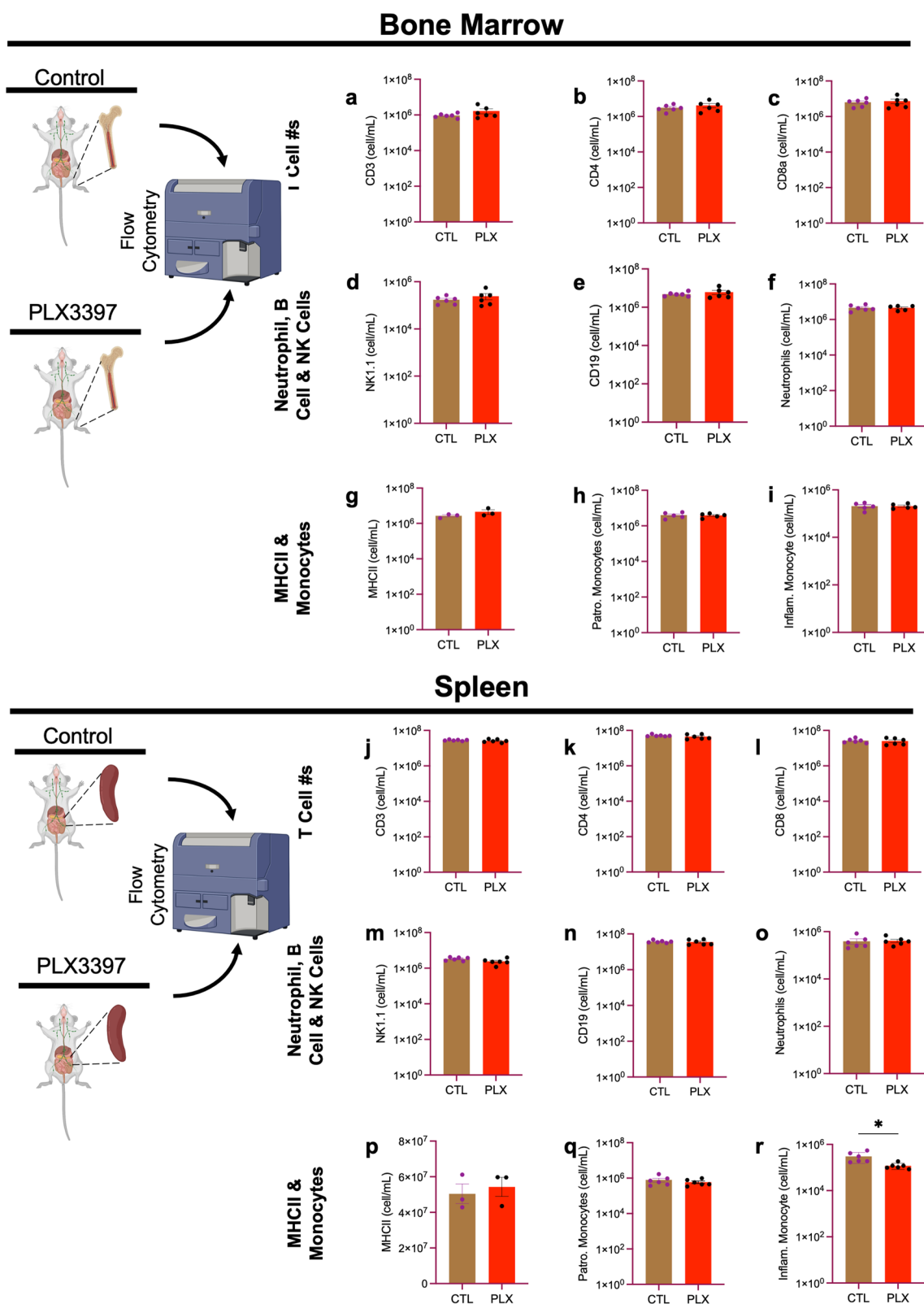


Fig. 2 (See legend on previous page.)

(Fig. 6b). In addition, except for M-CSF which was significantly increased in the PLX3397-fed group, all profiled brain cytokines were not altered in the homeostatic state with the high dose of PLX3397 for 7 days (Fig. 6c). Consequently, following LPS stimulation, we observed a significant decrease in TNF α , IL-1 α , and IL-1 β in the PLX3397-fed group; and an increase in M-CSF in the PLX3397-fed group (Fig. 6c).

We also ascertained to what extent PLX impacts cytokine secretion at 24 h after of LPS stimulation using Luminex assay (Additional file 2: Fig. S2a). Our results show that there was no significant difference between control and PLX3397-fed mice in the anti-inflammatory profile (IL-4, IL-13), except for IL-10 which was significantly reduced in PLX3397-fed mice compared to control (Additional file 2: Fig. S2b). We also observed a non-significant effect in the main pro-inflammatory profiles (IL-1 α , IL-1 β , TNF α , and IFN- γ) we examined. However, there was a significant increase in IL-6 in LPS-treated group compared to the normal saline group (Additional file 2: Fig. S2c). In addition, there was no significant difference in IL-6 secretion following LPS stimulation in both control and PLX3397-fed mice (Additional file 2: Fig. S2c). We observed that chemokine (CCL11, CXCL2, CXCL1, CCL5) secretion was not significantly impacted by PLX3397 following LPS stimulation. However, MIG (CXCL9) secretion was significantly decreased in PLX3397-fed mice following LPS stimulation compared to the control chow-fed mice (Additional file 2: Fig. S2d).

We next examined the effect of a high dose of PLX3397 on serum and brain downstream cellular signaling pathways. Our data show that PLX3397 alone or in combination with LPS did not significantly alter the total levels of any of the cellular (CREB, JNK, NF-kB, p38, ERK1/2, Akt, p70S6K, STAT3, STAT5) pathways we examined in both serum and brain (Additional file 3: Fig S3a, b). Our findings are congruent with previous data that reported that 50 mg/kg of PLX3397 every second day for three weeks does not alter the cellular production of pJNK and pERK1/2 in the visceral fat [49]. In all, our data show that CSF1R inhibition using PLX3397 does not impact peripheral immune cells' ability to secrete interleukins and chemokines both in the basal state and during Gram-negative bacterial infection.

PLX3977 does not block the sickness-inducing effects of LPS treatment

Given the evidence above that PLX3397 significantly depleted microglia and altered the expression of some inflammatory cytokines in an LPS-treatment context, we sought to investigate the possible roles of microglia in sickness behavior following LPS stimulation since the mice presented with sickness determinants despite the absence of microglia. Measurement of body weight and temperature are typically used to monitor the health or effects of anaphylactic symptoms in animals as one of the several determinants of sickness [22, 35, 41]. Our data show that a high dose of PLX3397 does not alter the body weight (Fig. 7a) and temperature (Fig. 7b). However, following LPS treatment both PLX3397-fed and control groups had a significant drop in body weight and temperature within 6 h compared to the normal saline-treated group (Fig. 7a, b). Several studies have shown that LPS in animals results in sickness behavior which is characterized by but not limited to decreased locomotor activity and appetite [7, 30, 36]. In the open field, the total distance traveled is often used as a measurement of sickness behavior in an inflammatory experimental paradigm. Our data show that PLX3397 at a high dose does not alter exploratory behavior in the open field (Fig. 7g). However, LPS treatment at 6 h significantly reduced the distance traveled (Fig. 7e), the movement velocity (Fig. 7f), and time in the center (Fig. 7g) compared to the normal saline-treated control group. Our data, therefore, suggest that in the absence of microglia, other cells are sufficient to mediate sickness behavior following LPS treatment.

Discussion

Microglia are the main innate immune cell in the CNS and have been implicated as a driving mechanism in several diseases of the nervous system. One approach to interrogate microglial roles in the CNS is to examine the consequence of microglial elimination on various aspects of CNS structure or function. Earlier techniques to eliminate microglia did so either *transiently*, e.g., by local administration of clodronate [38, 54, 69, 74], *pharmacogenetically* using diphtheria toxin or similar strategies [50, 58, 79] or *genetically* targeting genes for myeloid cell survival with developmental consequences as well as effects on other myeloid cells [5, 12,

(See figure on next page.)

Fig. 3 Immune cells in non-lymphoid organs (lung and kidney) are not altered by PLX3397. Bar graphs show the number of immune cells from the lungs: **a** CD3⁺, **b** CD4⁺, **c** CD8a⁺, **d** NK1.1⁺, **e** CD19⁺, **f** CD11b⁺Ly6G⁺, **g** CD11b⁺Ly6C^{high} (inflammatory monocytes), **h** CD11b⁺Ly6C^{low} (patrolling monocytes), **i** MHCII⁺; and the kidney: **j** CD3⁺, **k** CD4⁺, **l** CD8a⁺, **m** NK1.1⁺, **n** CD19⁺, **o** CD11b⁺Ly6G⁺, **p** CD11b⁺Ly6C^{high} (inflammatory monocytes), **q** CD11b⁺Ly6C^{low} (patrolling monocytes), **r** MHCII⁺. Data were analyzed with unpaired Student's *T*-test, *n* = 3 each, and data represented by mean \pm SEM

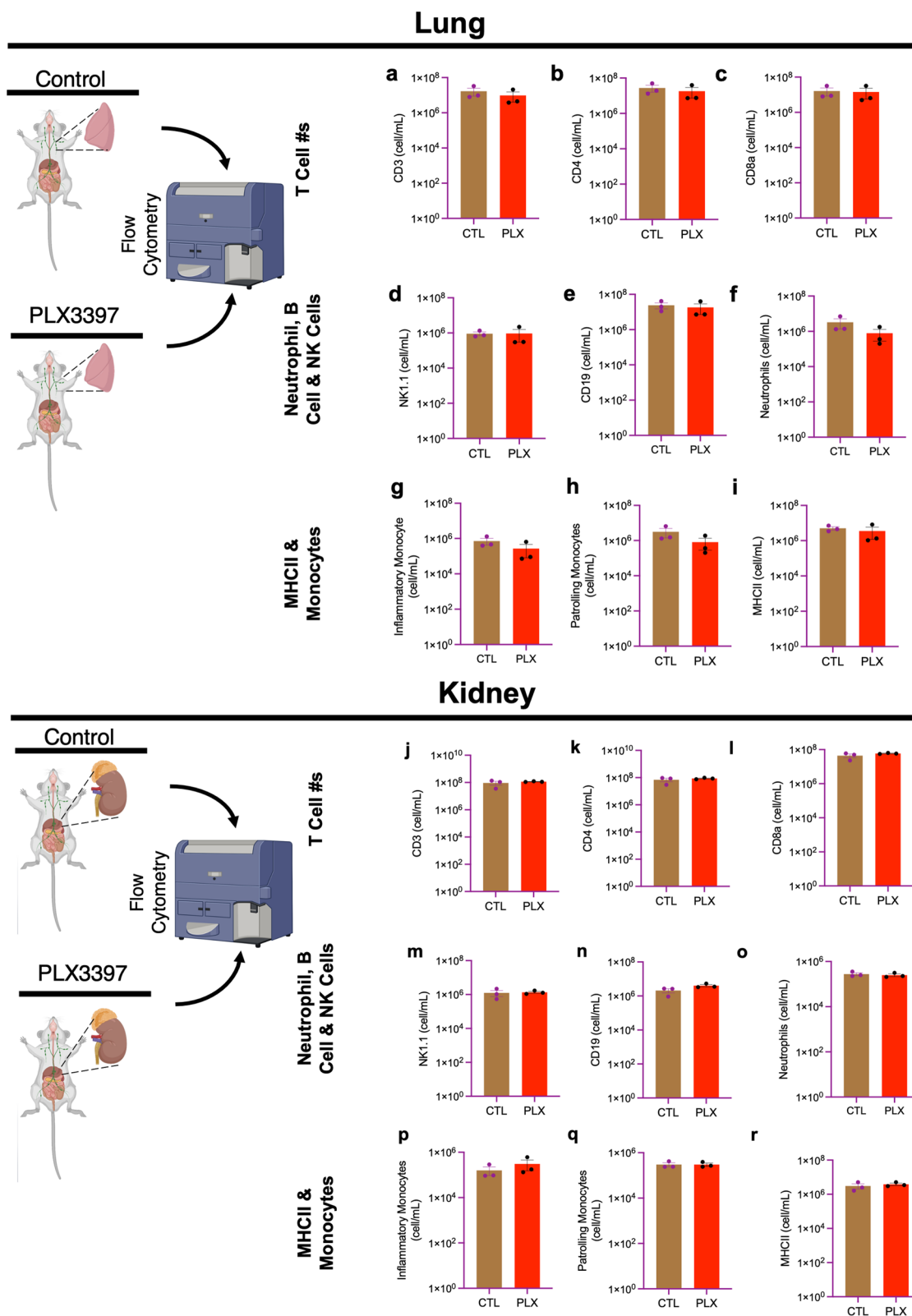


Fig. 3 (See legend on previous page.)

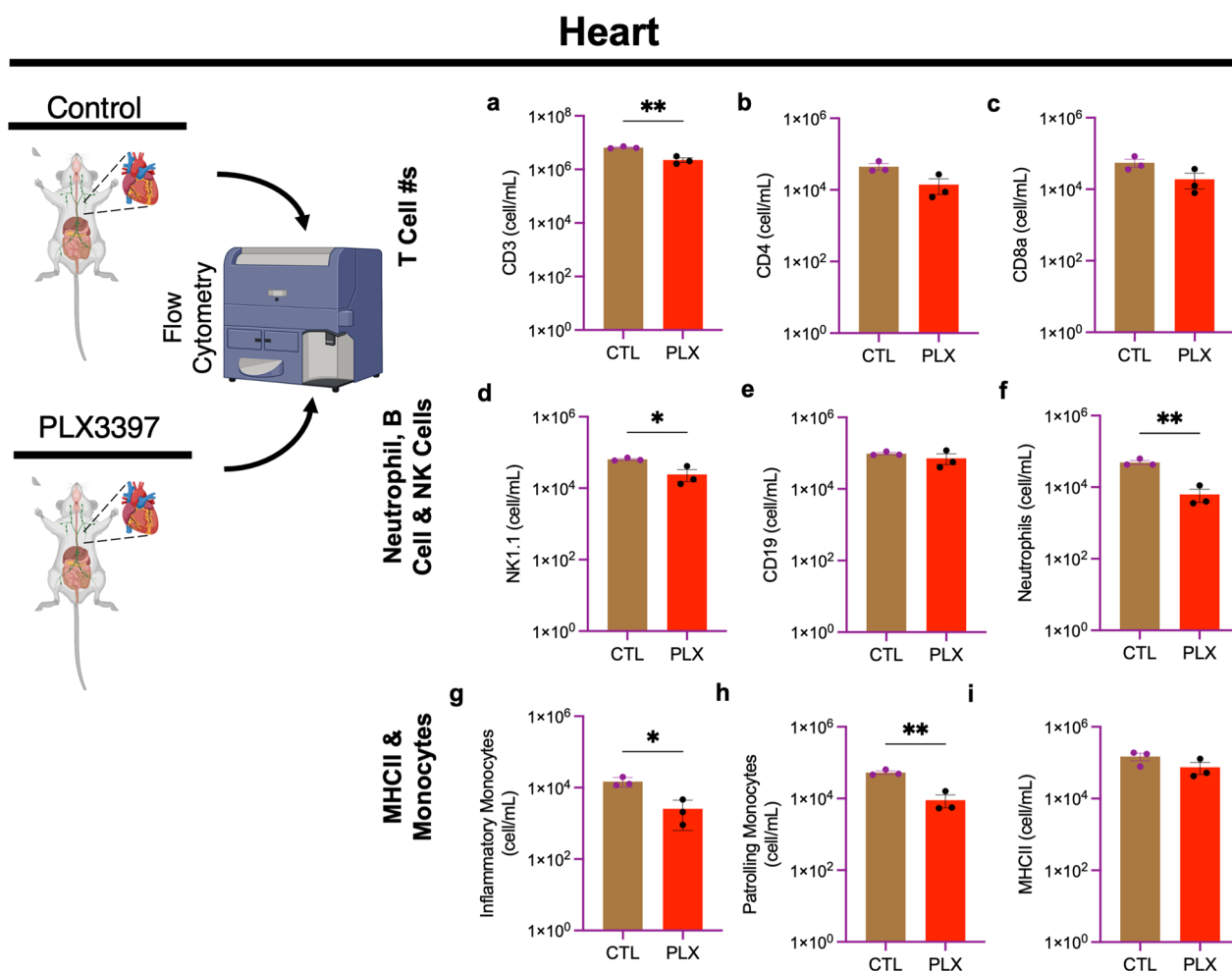


Fig. 4 PLX3397 has some minor effect on immune cell numbers in the heart. Bar graphs show the number of immune cells from the heart: **a** CD3⁺, **b** CD4⁺, **c** CD8a⁺, **d** NK1.1⁺, **e** CD19⁺, **f** CD11b⁺Ly6G⁺ (neutrophils), **g** CD11b⁺Ly6C^{high} (inflammatory monocytes), **h** CD11b⁺Ly6C_{low} (patrolling monocytes), **i** MHCII⁺. Data were analyzed with unpaired Student's *T*-test, *n* = 3, and data represented by mean ± SEM, **p* < 0.05, ***p* < 0.01

25, 48, 60]. Moreover, some of these techniques such as the pharmacogenetic ones have since been discovered to elicit indirect additional effects than microglial elimination in the brain. These include for example, physical alterations to the brain ventricles, increased glial reactivity, increased cytokine levels and some dysfunctional motor behaviors [4, 9, 59]. Therefore, these techniques suffer from elements of insufficient temporal control or unintended confounds in addition to eliminating microglia.

In 2014, with the introduction of the PLX family of CSF1R inhibitors as an alternative for microglial elimination, some of these concerns were mitigated by the approach to treat mice with these drugs through the chow feed which could allow for (1) temporal control (treatment could be commenced and terminated at will for short or long durations as needed), without (2) the known confounds of other approaches such as alterations to brain ventricle size, increased cytokine levels, astroglial activation and motor dysfunction [4, 9, 59].

(See figure on next page.)

Fig. 5 Innate immune cell numbers are negatively impacted by PLX3397 in lymphoid and non-lymphoid organs after LPS infection. Bar graphs show the number of immune cells from the spleen: **a** CD3⁺, **b** CD4⁺, **c** CD8a⁺, **d** NK1.1⁺, **e** CD19⁺, **f** CD11b⁺Ly6G⁺ (neutrophils), **g** CD11b⁺Ly6C^{high} (inflammatory monocytes), **h** CD11b⁺Ly6C_{low} (patrolling monocytes), **i** MHCII⁺; and the lung: **j** CD3⁺, **k** CD4⁺, **l** CD8a⁺, **m** NK1.1⁺, **n** CD19⁺, **o** CD11b⁺Ly6G⁺ (neutrophils), **p** CD11b⁺Ly6C^{high} (inflammatory monocytes), **q** CD11b⁺Ly6C_{low} (patrolling monocytes), **r** MHCII⁺. Data were analyzed with unpaired Student's *T*-test, *n* = 3–4, and data represented by mean ± SEM, **p* < 0.05, ***p* < 0.01

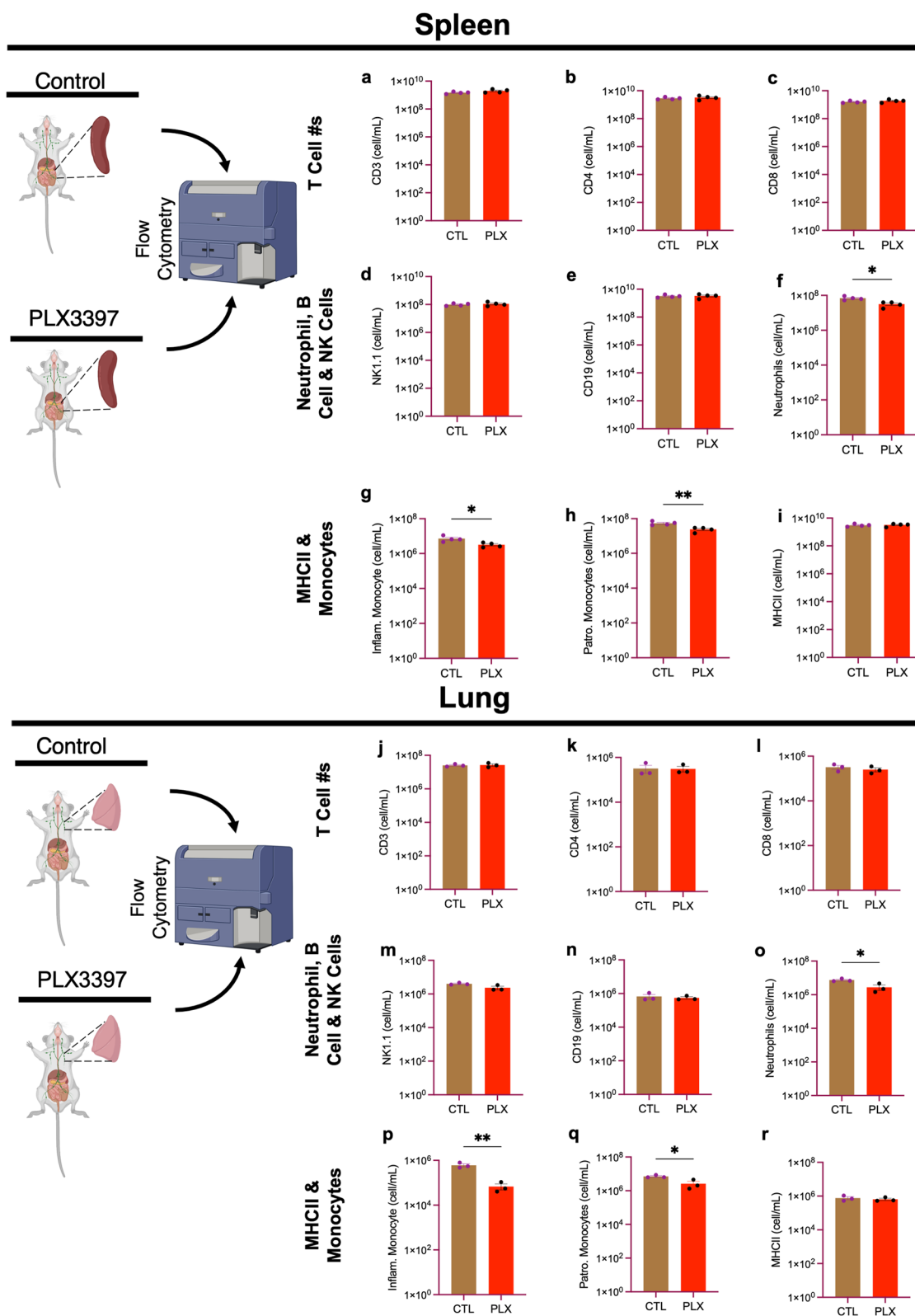


Fig. 5 (See legend on previous page.)

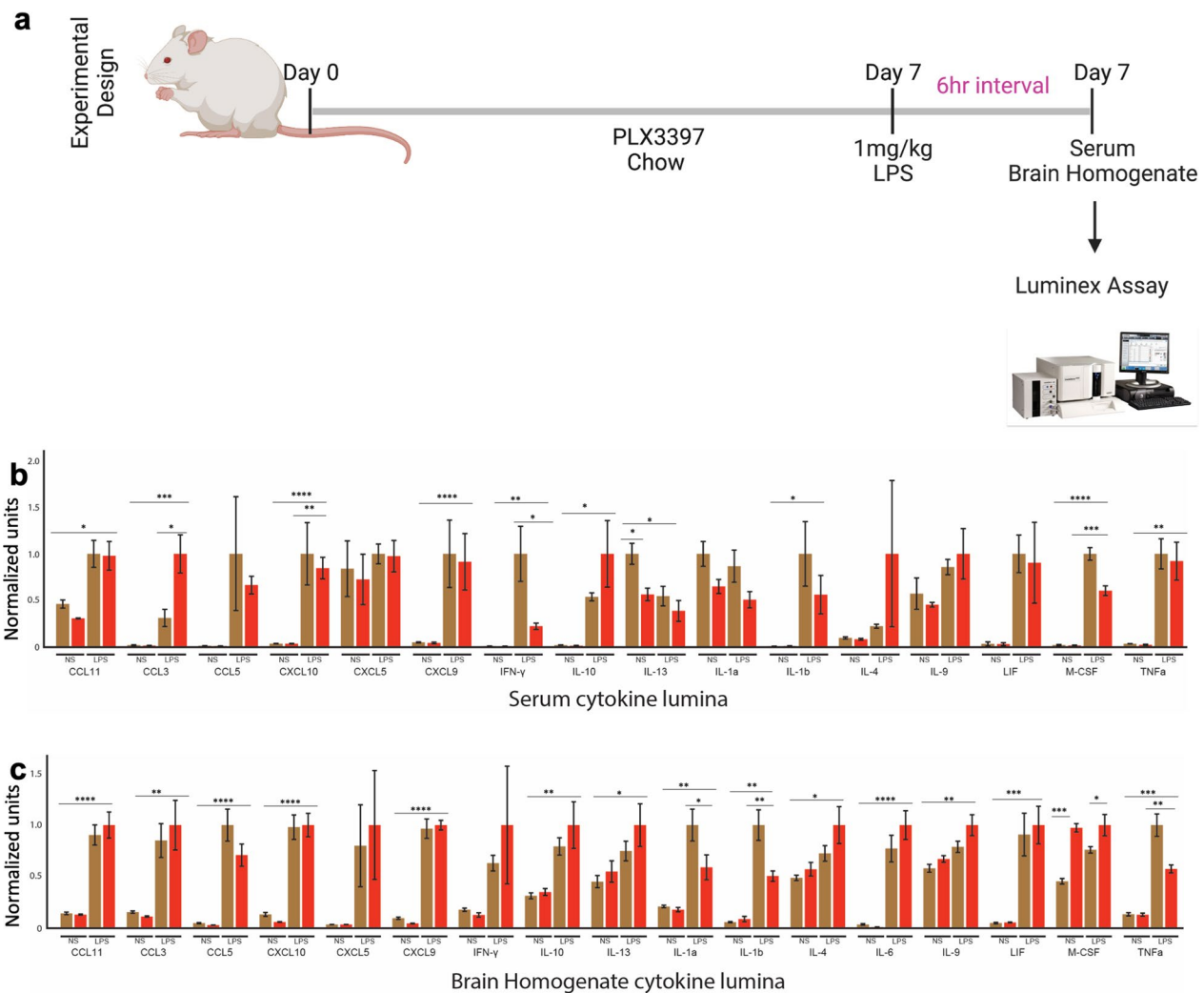


Fig. 6 PLX3397 decreases inflammatory cytokines in serum and brain homogenate following LPS. **a** Illustration of experimental design showing mice placed on PLX3397 for seven days followed by Luminex assay for serum and brain homogenate cytokine profiling. **b** serum cytokine profile **c** brain homogenate cytokine profile. Data were analyzed with unpaired Student's *T*-test, $n = 4-5$, and data represented by mean \pm SEM, * $p < 0.05$, ** $p < 0.01$. *** $p < 0.001$, **** $p < 0.0001$

However, recent studies suggests that PLX treatment has effects on the peripheral immune system including with cells outside the myeloid lineage such as B cells and T cells [43] raising a need to further characterize the effect of the PLX family of CSF1R antagonists. Here, we focused on the effects of PLX3397 rather than that for PLX5622 for four reasons. First, PLX3397 is more widely used in the literature (a PubMed search yields 293 results versus 170 for PLX5622). Second and possibly explaining the first reason, PLX3397 is more widely accessible to researchers because it is less expensive compared to PLX5622. Third, PLX3397 is used in more clinical trials (24 with several in 2020 and at least one in 2021 on the clinicaltrials.gov website) than PLX5622 (only 2 and the

last was in 2015) requiring a better understanding of its effects with its greater clinical use. Fourth, for basic science research, we were looking for an approach that rapidly eliminates microglia at low concentrations. The widely used concentration for PLX3397 is already high at 1200 mg/kg and that for PLX5622 was 290 mg/kg which we could increase to the maximum that has been used in the literature at 660 mg/kg. Thus, for experimental, financial, clinical, and practical reasons, we choose to conduct the study with PLX3397 though a study of PLX5622's effects would be just as good and is much needed. At this dose, we demonstrated effective microglial elimination within a relatively short duration of 7 days (Fig. 1). We selected this dose to provide a rapid and effective

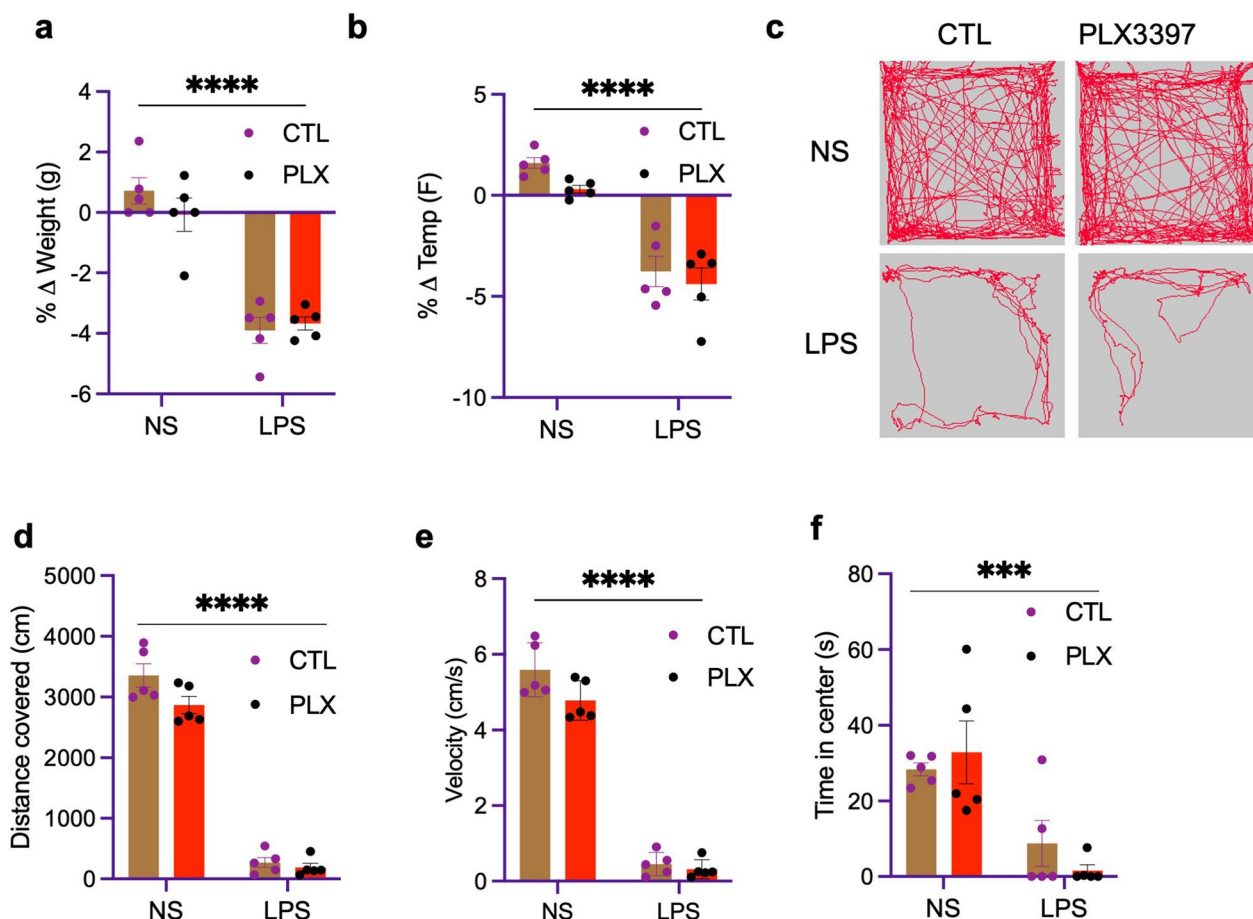


Fig. 7 PLX3397 does not affect LPS-induced sickness behavior. **a, b** Effects of LPS on **a** body weight and **b** body temperature measured 6 h after intraperitoneal LPS injection in PLX3397-fed mice compared to control chow-fed mice, **c** representative images of mouse exploration without and following LPS. **d-f** Quantification of locomotor activity measured by **d** distance traveled, **e** velocity and **f** time in center in an open-field test carried out 6 h post-LPS. Data represented by mean ± SEM, $n=5$, $***p < 0.001$, $****p < 0.0001$

depletion of microglia which we have used and confirmed in other previous from our lab [8, 24]. While lower doses could eliminate microglia by 2–3 weeks, we wanted a *rapid* elimination paradigm because some results from previous studies such as [44] have shown effects on the periphery which could result from a longer exposure to the diet. However, we had not previously examined the effects of this treatment regimen outside the brain.

We report that this regimen did not appreciably alter the peripheral immune cell profile in both lymphoid (Fig. 2) and non-lymphoid (Figs. 3, 4) organs, and cytokine profile in serum and brain in the basal state (Fig. 6). However, following LPS stimulation, we observed that innate immune cells from lymphoid and non-lymphoid organs were significantly decreased in the PLX3397-fed group (Fig. 5). In addition, we observed that PLX treatment coupled with LPS stimulation decreased the secretion of IFN- γ in serum and TNF α , IL-1 α , and IL-1 β in the brain (Fig. 6). However, these significantly

decreased secretions of inflammatory cytokines did not result in the alterations of downstream total protein levels of cellular signaling pathways (Additional file 2: Fig. S2). Furthermore, we demonstrated that pharmacological microglial depletion using PLX3397 did not abrogate sickness behavior in mice following LPS stimulation (Fig. 7), indicating that the peripheral immune system remains intact in the absence of microglia to mediate sickness behavior. Similar findings have recently been reported using PLX5622 in mice and microglial depletion induced by the administration of diphtheria toxin to Cx3cr1-Dtr transgenic rats [71]. Taken together, these findings suggest that PLX3397 at a dose of 660 mg/kg eliminates microglia by 7 days with little impact on peripheral immune cell numbers in the naïve state but limits the production of some innate immune cells in the periphery, and cytokine storm during a Gram-negative bacterial infection. Finally, we show that microglia are not required for sickness behavior. It is worth noting that our

studies leave open the possibility that the results found in the periphery following PLX3397 treatment to eliminate myeloid cells may result indirectly from consequences of microglial depletion or directly from PLX3397 effects in the periphery.

Microglial survival, maintenance, and proliferation are essentially dependent on CSF-1 and its receptor CSF1R. CSF1R is also expressed on peripheral immune cells specifically macrophages and monocytes. Elmore et al. [17] reported that PLX3397 at a dose of 290 mg/kg exerted a limited influence on other immune cells in the periphery. In addition, several other studies have reported inconsistency on the effect of PLX3397 on peripheral immune cells. Merry et al. [49] reported that PLX3397 (50 mg/kg) for 21 days through oral gavage significantly decreased the numbers of macrophages in the adipose tissue, but not of circulating myeloid cells. Szalay et al. [66] reported that PLX3397 (290 mg/kg) in feed for 21 days did not alter monocyte/granulocyte and lymphocyte populations in both blood and spleen. Other studies have also indicated that PLX3397 results in a significant reduction in red blood cells, hemoglobin, platelets, dendritic cells, Ly6C⁻ monocytes [61], and splenic red pulp macrophages [29]. A plausible interpretation of these results may be due to the different concentrations, duration, and routes of administration of PLX3397 treatment and possible differences in vivarium used in these studies.

In addition, PLX5622, a more specific CSF1R inhibitor has also been shown to significantly deplete macrophages and monocytes in both the circulation and the liver [75]. Another study using PLX5622 suggested it is not CNS-specific, with long-term effects on the myeloid and lymphoid compartments of bone marrow, spleen, and blood [43]. In contrast, our results show that the numbers of immune cells from both myeloid and lymphoid compartments were not impacted by PLX3397 at a concentration of 660 mg/kg for 7 days. However, upon stimulation with LPS, we observed a significant decrease in immune cells of the myeloid compartment specifically neutrophils, classical and non-classical monocytes in both lymphoid and non-lymphoid organs. These results suggest that each study using these drugs should specifically analyze the peripheral immune compartment to clarify effects from the route of delivery, duration of treatment and concentration of drug used.

Some limitations of the current study are noteworthy. First, while we did not find significant effects of PLX3397 treatment on peripheral immune cells, microglia are not the only myeloid cells eliminated with a PLX3397 treatment. Indeed, border associated (meningeal and perivascular) macrophages are also eliminated with PLX3397 treatment (data not shown) requiring caution in assuming microglial specificity among brain macrophages

when using PLX3397. Second, our study was strictly limited to the depletion paradigm, though there is an established paradigm of repopulation that ensues upon PLX3397 drug withdrawal that could also have impacts on brain and peripheral immune cell density that would be worth investigating in future since it has now been shown in several paradigms that following repopulation in aged mice, improvements in neuronal function [18] and recovery from pathology [29, 45, 62] are evident. Whether these can be a result of changes to peripheral cell populations, however, has not been investigated in those paradigms nor in our paradigm. Third, our analysis was done on groups of 3–6 mice and we acknowledge that our study would be improved by increasing the number of mice per group. Fourth, we used a specific LPS-treatment paradigm of a single dose at 1 mg/kg and examination at a single timepoint at 24 h. We report our findings here but also acknowledge that other LPS treatment concentrations and timepoints may yield different results. Finally, while we show limited effects on peripheral immune cell density during PLX3397 treatment, we did not assess the function of these immune populations and thus cannot rule out functional consequences to these cell populations independent of effects on density. All these limitations are of course of interest for future studies.

In conclusion, in the current study, we report a brain-selective effect of a 7-day 660 mg/kg PLX3397 treatment on the myeloid cell population when compared to peripheral lymphoid (bone marrow and spleen) and non-lymphoid (kidney, lung, and heart) organs. PLX3397 at this concentration and for this duration had minimal effects on various immune cell populations in these organs in the naïve state. However, following LPS-induced infection, PLX3397 treatment at this concentration and duration resulted in a reduction in the number of some immune cell populations in the periphery. These results provide a paradigm that could be of use for further studies in which PLX3397 is used.

Materials and methods

Animals

All animal experimentations were carried out in accordance with the relevant guidelines and regulations of the University of Virginia and approved by the Institutional Animal Care and Use Committee with protocol number 4237. The animals were housed under controlled temperature, humidity, and light (12:12 h. light: dark cycle), with food and water readily available ad libitum. Only male mice were used for this study on a C57BL/6J background age 11–13 weeks and consisted of the following genotypes: CX3CR1^{GFP/+} expressing GFP under control of the fractalkine receptor (CX3CR1) promoter [34] and

C57Bl/6J mice as wildtype mice. Mice were housed in groups for the experiment without special environmental enrichment.

Pharmacological elimination of microglia

Microglia were depleted using a potent CSF1R inhibitor, PLX3397, that has been previously shown to lack inflammatory consequences during the elimination process. Microglia from the adult brain were depleted by feeding adult mice with chow containing PLX3397 (660 mg/kg) in the experimental group and control chow containing 75 mg/kg PLX3397 for 7 days. We recently showed that at 75 mg/kg, PLX3397 did not affect microglial numbers in the brain [24].

Open field behavioral test

The open field test was carried out in a custom-built arena using a white plastic material with 35 (L)×35 (B)×21 (H) cm dimensions. Mouse cages were moved into the testing room and allowed to acclimate for 1 h. Illumination in the room was maintained at 150 Lux intensity, temperature, and relative humidity were also relatively constant at 70.2±0.9 °F and 40.9±5%, respectively. All experiments were done during the light cycle. Five mice from the same cage were simultaneously placed into different arenas that had been cleaned with 70% ethanol. Each mouse was placed adjacent to the wall of the arena and allowed to freely explore the space. Their open field activities (horizontal locomotion and mobility) in the arenas were video monitored for 10 min using EthoVision[®] XT (Noldus, Wageningen, The Netherlands), and then subsequently tracked offline for activity analysis using the same software.

Lipopolysaccharide administration

To evaluate the effect of LPS on the immune profile, mice placed on a high dose of PLX3379 for 7 days were weighed using an electronic scale (CGOLDENWALL) before and 6 h after i.p injection of 1 mg/kg/bw of LPS prepared from *Escherichia coli* (026:B6, Sigma-Aldrich, St. Louis, USA). Body temperature was also recorded before and after LPS injection using a hand-held medical infra-red thermometer (Model: HG01, China) as previously described [35].

Cytokine and cell signaling assay

Following 6 h of LPS injections, mice were subjected to cardiac puncture. The blood collected was allowed to coagulate for 30 min at room temperature and subsequently centrifuged for 10 min at 1000×g. The supernatant (serum) was collected and stored at – 80 °C until ready for the Luminex assay. Spleen and lungs were also collected and prepared for flow cytometric staining to

profile peripheral immune cells. A different cohort of mice was perfused with ice-cold 1X PBS, the brain was quickly removed and homogenized. The supernatant was collected and stored at – 80 °C until ready for Luminex assay. Milliplex mouse cytokine/chemokine magnetic bead analysis kit was obtained from Millipore Sigma (MA, USA). For cellular kinases, Milliplex multi-pathway 9-plex magnetic bead kit (48-680MG) was used. Assays were run in duplicate according to the manufacturer's protocol. Data were collected using the Luminex Intelliflex (Luminex, Austin, TX, USA). Data analysis was performed using the Milliplex Analyst 5.1 software (MA, USA). The multi-pathway 9-plex data were normalized to GAPDH.

Tissue preparation and immunostaining

For confocal microscopy studies, mice were euthanized with CO₂ and transcardially perfused with sodium phosphate buffer (PBS; 50 mM at pH 7.4) followed by 4% paraformaldehyde (PFA). All perfusion solutions were chilled on ice prior to use. We used a perfusion pump (Masterflex[®] Ismatec[®]) at a perfusion flow rate of 7 mL/min. Brains were then fixed in 4% PFA overnight. Using a vibratome (Leica VT100S), 40-µm-thick sections of the brain were cut in chilled PBS. Slices were then stored in cryoprotectant (40% PBS, 30% ethylene glycol, and 30% glycerol) at –20 °C while further processing took place. Brain sections containing the ventral hippocampus CA1 (Bregma –3.27 and –4.03), the frontal cortex (Bregma 2.93 and –2.57), and the sensorimotor cortex (Bregma –2.5 and +2.0) were examined.

Fluorescence microscopy

Fluorescently immunolabelled brain sections were imaged with a Leica SP8 Laser Confocal Microscope. Image analysis to quantify microglia cell numbers through z-stacks was done using ImageJ. Microglia cell number was automatically counted using the ImageJ cell counter plugin.

Tissue processing and flow cytometry staining

Mice were euthanized with CO₂ and sprayed with 70% ethanol. The spleen was collected and placed in cold complete RPMI media (cRPMI) (10% FBS, 1% sodium pyruvate, 1% non-essential amino acids, 1% penicillin/streptomycin, 0.1% 2-ME). The spleen was mashed through a 40-µm filter in 50 mL conical using a syringe plunger and wash through with 15-mL cRPMI. The suspension was centrifuged at 1600 rpm for 5 min at 4 °C using Eppendorf Centrifuge 5804R with an S-4–72 rotor. The spleen was resuspended in 2 mL RBC lysis buffer for 2 min and the reaction was stopped by adding 13 mL

cRPMI. The suspension was once again centrifuged, and the resulting pellet was resuspended in 5 mL cRPMI and kept on ice.

For the preparation of a single-cell suspension for the bone marrow, the femur and tibia were carefully removed without splintering them to obtain the bone marrow. The bones were placed in a petri dish containing 70% ethanol for 1–2 min to disinfect and transferred to a petri dish containing 4 mL cRPMI on ice. The femora and tibiae were flushed with 10 mL ice-cold cRPMI using a 21G needle attached to a 10-mL syringe. A single-cell suspension was generated by gently triturating the cells through the needle until large clumps were no longer present and the suspension was run through a 40 μ m filter in a 50 mL conical tube. The suspension was centrifuged at 1600 rpm for 5 min at 4 °C. The bone marrow was resuspended in 2 mL RBC lysis buffer for 2 min and the reaction was stopped by adding 13 mL cRPMI. The suspension was centrifuged at 1600 rpm for 5 min at 4 °C, the supernatant was aspirated, and the pellet was resuspended in 5 mL cRPMI.

For the preparation of single cells from the kidney, an established protocol was used [47]. Briefly, following mice euthanizer with CO₂, they were exsanguinated. Both kidneys were removed after careful renal pedicle dissection and decapsulated. Kidneys were finely minced and incubated in collagenase D (2 mg/mL, Sigma-Aldrich, St. Louis, MO, USA) for 30 min at 37 °C. Single-cell of the kidney was prepared by straining through a 70 μ m strainer (Corning).

For the preparation of single-cell suspension from the heart and lung, we adopted previously published protocols [11, 23, 26, 42, 80]. Following euthanizer with CO₂ and systemic perfusion with ice cold 1 \times PBS, organs of choice were carefully dissected and cut into 1–2 mm pieces and incubated for 30 min in cRPMI containing 2 mg/mL collagenase D at 37 °C. Digested tissue was strained using 70 μ m strainer. After washing with cRPMI, cell suspension was then run at room temperature with isotonic Percoll density (GE Healthcare, Chicago, IL, USA) centrifugation (1500 \times g for 30 min in brake-off mode). Collected cells from each organ were washed and resuspended on cRPMI.

Following the generation of a single-cell suspension, cells were counted using automated cell counter (C100, RWD, China), 150 μ L (~1 \times 10E6) of each sample were placed in a 96-well plate and incubated for 10 min in 50 μ L Fc block (1:1000, CD16/32, Clone 93, eBioscience) at room temperature. Cells were then incubated in primary antibodies at a concentration of 1:200 and fixable viability dye eFluor 506 (eBioscience) at a concentration of 1:800 for 30 min at 4 °C. Antibody clones used for experiments included: NK1.1 (PK136), CD3e (145–2C11), CD8a

(53–6.7), CD4 (RM4–5), CD19 (eBio 1D3), Ly6C (HK1.4), F4/80 (BM8), CD11b (M1/70), Ly6G (1A8), CD45 (30-F11), MHC II (M5/114.15.2), and CD11c (N418) (Invitrogen). After staining, cells were washed twice and fixed overnight in 2% PFA at 4 °C. Cells were washed twice with cell staining buffer (BioLegend, Cat. # 420201) and transferred into a 5 mL Polystyrene round-bottom tube with cell-strainer cap tubes (Falcon), then were analyzed on a Gallios flow cytometer (Beckman-Coulter) by gating on 250,000 live events. Flow cytometry data were analyzed using FlowJo (version 10.8.1).

Statistical analysis

Data were initially measured for normality and homoscedasticity and upon comparing normal distributions and variances further analyzed with the respective tests. Student's t-test was used to compare two groups. Other comparisons were evaluated using two-way ANOVA (experiments with 2 variables), followed by Tukey post hoc test for multiple comparisons within the tested groups.

Supplementary Information

The online version contains supplementary material available at <https://doi.org/10.1186/s12974-023-02924-5>.

Additional file 1: Fig S1: Gating strategy employed in peripheral immune cell population profiling. C57BL6/J mice were fed a chow diet for 7 days containing CSF1R inhibitor PLX3397 (660 mg/kg). Samples were labeled with mixtures of specific antibodies against immune cell populations and subjected to flow cytometric analysis. Singlets were gated FS-A/FS-H, live mononuclear cells were gated based on SS-A/fixable Viability Dye (eFluor 506), then size gated based on SS-A/FS-A to exclude red blood cells. As indicated in the illustration above, a specific population of choice based on the antibody was identified from the size gate.

Additional file 2: Figure S2. Seven days of CSF1R inhibition with PLX3397 does not alter serum cytokine/chemokine profile (except IL-10 and CXCL9) 24 h after LPS stimulation. **a.** Illustration of experimental design showing mice placed on PLX3397 for seven days followed by serum Luminex assay for cytokine profiling. **b.** serum cytokine anti-inflammatory profile **c.** serum cytokine pro-inflammatory profile **d.** serum chemokine profile. Data were analyzed with unpaired Student's T-test, n = 3–5, and data represented by mean \pm SEM, *p < 0.05, **p < 0.01, ***p < 0.001, ****p < 0.0001.

Additional file 3: Figure S3. PLX3397 does not affect cellular kinases in serum and brain homogenate following LPS infection. **a.** serum cellular kinases pathways **b.** brain homogenates cellular kinase pathways. Data were analyzed with Student's unpaired T-tests, n = 5, and data represented by mean \pm SEM.

Acknowledgements

The authors would like to appreciate members of Eyo Lab, Center for Brain Immunology and Glia (BIG) at the University of Virginia for their input in this work. We would also like to thank the UVA Flow Cytometry Core for methodological assistance. Parts of some figures were created with Biorender.com.

Author contributions

AKO and UBE designed the experiments; AKO, JOU, MAC, and VDC performed the experiments; SL analyzed some of the data. The original draft was written

by AKO; UBE reviewed and revised the draft, and the final version was read and approved by all authors.

Funding

This work was supported by funding from The National Institute of Health (R01NS122782 and R01NS119243) and The Owens Family Foundation.

Availability of data and materials

All datasets used and/or analyzed in this present study are available from the corresponding author upon request.

Declarations

Ethics approval and consent to participate

All procedures were performed in accordance with the National Institutes of Health Guideline for the Care and Use of Laboratory Animals and approved by the Institutional Animal Care and Use Committee of the University of Virginia (IACUC no: 4237).

Competing interests

The authors declare no competing interests.

Received: 6 June 2023 Accepted: 10 October 2023

Published online: 21 October 2023

References

- Akira S. Toll-like receptor signaling. *J Biol Chem*. 2003;278(40):38105–8. <https://doi.org/10.1074/jbc.R300028200>.
- Alliot F, Godin I, Pessac B. Microglia derive from progenitors, originating from the yolk sac, and which proliferate in the brain. *Brain Res Dev Brain Res*. 1999;117(2):145–52. [https://doi.org/10.1016/s0165-3806\(99\)00113-3](https://doi.org/10.1016/s0165-3806(99)00113-3).
- Amanati A, Sajedianfard S, Khajeh S, Ghasempour S, Mehrangiz S, Nematollahi S, Shahhoseini Z. Bloodstream infections in adult patients with malignancy, epidemiology, microbiology, and risk factors associated with mortality and multi-drug resistance. *BMC Infect Dis*. 2021;21(1):636. <https://doi.org/10.1186/s12879-021-06243-z>.
- Bedolla A, Taranov A, Luo F, Wang J, Turcato F, Fugate EM, Greig NH, Lindquist DM, Crone SA, Goto J, Luo Y. Diphtheria toxin induced but not CSF1R inhibitor mediated microglia ablation model leads to the loss of CSF/ventricular spaces in vivo that is independent of cytokine upregulation. *J Neuroinflammation*. 2022;19(1):3. <https://doi.org/10.1186/s12974-021-02367-w>.
- Beers DR, Henkel JS, Xiao Q, Zhao W, Wang J, Yen AA, Siklos L, McKercher SR, Appel SH. Wild-type microglia extend survival in PU.1 knockout mice with familial amyotrophic lateral sclerosis. *Proc Natl Acad Sci USA*. 2006;103(43):16021–6. <https://doi.org/10.1073/pnas.0607423103>.
- Bhat S, Muthunatarajan S, Mulki SS, Archana Bhat K, Kotian KH. Bacterial infection among cancer patients: analysis of isolates and antibiotic sensitivity pattern. *Int J Microbiol*. 2021;2021:8883700. <https://doi.org/10.1155/2021/8883700>.
- Biesmans S, Meert TF, Bouwknecht JA, Acton PD, Davoodi N, De Haes P, Kuijlaars J, Langlois X, Matthews LJ, Ver Donck L, Hellings N, Nuydens R. Systemic immune activation leads to neuroinflammation and sickness behavior in mice. *Mediators Inflamm*. 2013;2013: 271359. <https://doi.org/10.1155/2013/271359>.
- Bisht K, Okojie KA, Sharma K, Lentferink DH, Sun YY, Chen HR, Uweru JO, Amancherla S, Caltuttawala Z, Campos-Salazar AB, Corliss B, Jabbour L, Benderoth J, Friestad B, Mills WA 3rd, Isakson BE, Tremblay ME, Kuan CY, Eyo UB. Capillary-associated microglia regulate vascular structure and function through PANX1-P2RY12 coupling in mice. *Nat Commun*. 2021;12(1):5289. <https://doi.org/10.1038/s41467-021-25590-8>.
- Bruttger J, Karam K, Wortge S, Regen T, Marini F, Hoppmann N, Klein M, Blank T, Yona S, Wolf Y, Mack M, Pinteaux E, Muller W, Zipp F, Binder H, Bopp T, Prinz M, Jung S, Waissman A. Genetic cell ablation reveals clusters of local self-renewing microglia in the mammalian central nervous system. *Immunity*. 2015;43(1):92–106. <https://doi.org/10.1016/j.immuni.2015.06.012>.
- Cannarile MA, Weisser M, Jacob W, Jegg AM, Ries CH, Ruttinger D. Colony-stimulating factor 1 receptor (CSF1R) inhibitors in cancer therapy. *J Immunother Cancer*. 2017;5(1):53. <https://doi.org/10.1186/s40425-017-0257-y>.
- Couter CJ, Surana NK. Isolation and flow cytometric characterization of murine small intestinal lymphocytes. *J Vis Exp*. 2016;111. <https://doi.org/10.3791/54114>.
- Cronk JC, Filiano AJ, Louveau A, Marin I, Marsh R, Ji E, Goldman DH, Smirnov I, Geraci N, Acton S, Overall CC, Kipnis J. Peripherally derived macrophages can engraft the brain independent of irradiation and maintain an identity distinct from microglia. *J Exp Med*. 2018;215(6):1627–47. <https://doi.org/10.1084/jem.20180247>.
- Csaszar E, Lenart N, Cserep C, Kornyei Z, Fekete R, Posfai B, Balazsfi D, Hangya B, Schwarcz AD, Szabadits E, Szollosi D, Zsigeti K, Mathe D, West BL, Sviatko K, Bras AR, Mariani JC, Kliewer A, Lenkei Z, Hricisak L, Benyó Z, Baranyi M, Sperlág B, Menyhart Á, Eszter F, Denes A. Microglia modulate blood flow, neurovascular coupling, and hypoperfusion via purinergic actions. *J Exp Med*. 2022;219(3):e20211071. <https://doi.org/10.1084/jem.20211071>.
- Dal Lin C, Tona F, Osto E. The heart as a psychoneuroendocrine and immunoregulatory organ. *Adv Exp Med Biol*. 2018;1065:225–39. https://doi.org/10.1007/978-3-319-77932-4_15.
- Dal Lin C, Tona F, Osto E. The crosstalk between the cardiovascular and the immune system. *Vasc Biol*. 2019;1(1):H83–8. <https://doi.org/10.1530/VB-19-0023>.
- Davalos D, Grutzendler J, Yang G, Kim JV, Zuo Y, Jung S, Littman DR, Dustin ML, Gan WB. ATP mediates rapid microglial response to local brain injury in vivo. *Nat Neurosci*. 2005;8(6):752–8. <https://doi.org/10.1038/nn1472>.
- Elmore MR, Najafi AR, Koike MA, Dagher NN, Spangenberg EE, Rice RA, Kitazawa M, Matusow B, Nguyen H, West BL, Green KN. Colony-stimulating factor 1 receptor signaling is necessary for microglia viability, unmasking a microglia progenitor cell in the adult brain. *Neuron*. 2014;82(2):380–97. <https://doi.org/10.1016/j.neuron.2014.02.040>.
- Elmore MRP, Hohsfield LA, Kramar EA, Soreq L, Lee RJ, Pham ST, Najafi AR, Spangenberg EE, Wood MA, West BL, Green KN. Replacement of microglia in the aged brain reverses cognitive, synaptic, and neuronal deficits in mice. *Aging Cell*. 2018;17(6): e12832. <https://doi.org/10.1111/acel.12832>.
- Erblich B, Zhu L, Etgen AM, Dobrenis K, Pollard JW. Absence of colony stimulation factor-1 receptor results in loss of microglia, disrupted brain development and olfactory deficits. *PLoS ONE*. 2011;6(10): e26317. <https://doi.org/10.1371/journal.pone.0026317>.
- Eyo UB, Peng J, Swiatkowski P, Mukherjee A, Bispo A, Wu LJ. Neuronal hyperactivity recruits microglial processes via neuronal NMDA receptors and microglial P2Y12 receptors after status epilepticus. *J Neurosci*. 2014;34(32):10528–40. <https://doi.org/10.1523/JNEUROSCI.0416-14.2014>.
- Fantin A, Vieira JM, Gestri G, Denti L, Schwarz Q, Prykhodzhiy S, Peri F, Wilson SW, Ruhrberg C. Tissue macrophages act as cellular chaperones for vascular anastomosis downstream of VEGF-mediated endothelial tip cell induction. *Blood*. 2010;116(5):829–40. <https://doi.org/10.1182/blood-2009-12-257832>.
- Finkelmann FD. Anaphylaxis: lessons from mouse models. *J Allergy Clin Immunol*. 2007;120(3):506–15. <https://doi.org/10.1016/j.jaci.2007.07.033>. (quiz 516–507).
- Geem D, Medina-Contreras O, Kim W, Huang CS, Denning TL. Isolation and characterization of dendritic cells and macrophages from the mouse intestine. *J Vis Exp*. 2012;63:e4040. <https://doi.org/10.3791/4040>.
- Gibbs-Shelton S, Benderoth J, Gaykema RP, Straub J, Okojie KA, Uweru JO, Lentferink DH, Rajbanshi B, Cowan MN, Patel B, Campos-Salazar AB, Perez-Reyes E, Eyo UB. Microglia play beneficial roles in multiple experimental seizure models. *Glia*. 2023. <https://doi.org/10.1002/glia.24364>.
- Ginhoux F, Greter M, Leboeuf M, Nandi S, See P, Gokhan S, Mehler MF, Conway SJ, Ng LG, Stanley ER, Samokhvalov IM, Merad M. Fate mapping analysis reveals that adult microglia derive from primitive macrophages. *Science*. 2010;330(6005):841–5. <https://doi.org/10.1126/science.1194637>.
- Ginhoux F, Liu K, Helft J, Bogunovic M, Greter M, Hashimoto D, Price J, Yin N, Bromberg J, Lira SA, Stanley ER, Nussenzweig M, Merad M. The origin and development of nonlymphoid tissue CD103+ DCs. *J Exp Med*. 2009;206(13):3115–30. <https://doi.org/10.1084/jem.20091756>.
- Greter M, Lelios I, Pelczar P, Hoeffel G, Price J, Leboeuf M, Kundig TM, Frei K, Ginhoux F, Merad M, Becher B. Stroma-derived interleukin-34 controls the development and maintenance of Langerhans cells and the

- maintenance of microglia. *Immunity*. 2012;37(6):1050–60. <https://doi.org/10.1016/j.immuni.2012.11.001>.
28. Han J, Sarlius H, Wszolek ZK, Karrenbauer VD, Harris RA. Microglial replacement therapy: a potential therapeutic strategy for incurable CSF1R-related leukoencephalopathy. *Acta Neuropathol Commun*. 2020;8(1):217. <https://doi.org/10.1186/s40478-020-01093-3>.
 29. Han JM, Fan YS, Zhou K, Zhu KY, Blomgren K, Lund H, Zhang XM, Harris RA. Underestimated peripheral effects following pharmacological and conditional genetic microglial depletion. *Int J Mol Sci*. 2020;21(22):8603. <https://doi.org/10.3390/ijms21228603>.
 30. Hart BL. Biological basis of the behavior of sick animals. *Neurosci Biobehav Rev*. 1988;12(2):123–37. [https://doi.org/10.1016/s0149-7634\(88\)80004-6](https://doi.org/10.1016/s0149-7634(88)80004-6).
 31. Haupt F, Krishnasamy K, Napp LC, Augustynik M, Limbourg A, Gam-rekeshvili J, Bauersachs J, Haller H, Limbourg FP. Retinal myeloid cells regulate tip cell selection and vascular branching morphogenesis via Notch ligand Delta-like 1. *Sci Rep*. 2019;9(1):9798. <https://doi.org/10.1038/s41598-019-46308-3>.
 32. Hughes CE, Nibbs RJB. A guide to chemokines and their receptors. *FEBS J*. 2018;285(16):2944–71. <https://doi.org/10.1111/febs.14466>.
 33. Jin WN, Shi SX, Li Z, Li M, Wood K, Gonzales RJ, Liu Q. Depletion of microglia exacerbates postischemic inflammation and brain injury. *J Cereb Blood Flow Metab*. 2017;37(6):2224–36. <https://doi.org/10.1177/0271678X17694185>.
 34. Jung S, Aliberti J, Graemmel P, Sunshine MJ, Kreutzberg GW, Sher A, Littman DR. Analysis of fractalkine receptor CX(3)CR1 function by targeted deletion and green fluorescent protein reporter gene insertion. *Mol Cell Biol*. 2000;20(11):4106–14. <https://doi.org/10.1128/MCB.20.11.4106-4114.2000>.
 35. Kawakami Y, Sielski R, Kawakami T. Mouse body temperature measurement using infrared thermometer during passive systemic anaphylaxis and food allergy evaluation. *J Vis Exp*. 2018; (139). <https://doi.org/10.3791/58391>.
 36. Kent S, Bluthe RM, Kelley KW, Dantzer R. Sickness behavior as a new target for drug development. *Trends Pharmacol Sci*. 1992;13(1):24–8. [https://doi.org/10.1016/0165-6147\(92\)90012-u](https://doi.org/10.1016/0165-6147(92)90012-u).
 37. Kierdorf K, Erny D, Goldmann T, Sander V, Schulz C, Perdiguero EG, Wieghofer P, Heinrich A, Riemke P, Holscher C, Muller DN, Luckow B, Brocker T, Debowski K, Fritz G, Odenakker G, Diefenbach A, Biber K, Heikenwalder M, Geissmann F, Rosenbauer F, Prinz M. Microglia emerge from erythromyeloid precursors via Pu.1- and Irf8-dependent pathways. *Nat Neurosci*. 2013;16(3):273–80. <https://doi.org/10.1038/nn.3318>.
 38. Kohl A, Dehghani F, Korff HW, Hailer NP. The bisphosphonate clodronate depletes microglial cells in excitotoxically injured organotypic hippocampal slice cultures. *Exp Neurol*. 2003;181(1):1–11. [https://doi.org/10.1016/s0014-4886\(02\)00049-3](https://doi.org/10.1016/s0014-4886(02)00049-3).
 39. Kumar V. Pulmonary innate immune response determines the outcome of inflammation during pneumonia and sepsis-associated acute lung injury. *Front Immunol*. 2020;11:1722. <https://doi.org/10.3389/fimmu.2020.01722>.
 40. Lawson LJ, Perry VH, Dri P, Gordon S. Heterogeneity in the distribution and morphology of microglia in the normal adult mouse brain. *Neuroscience*. 1990;39(1):151–70. [https://doi.org/10.1016/0306-4522\(90\)90229-w](https://doi.org/10.1016/0306-4522(90)90229-w).
 41. Lee JK, Vadas P. Anaphylaxis: mechanisms and management. *Clin Exp Allergy*. 2011;41(7):923–38. <https://doi.org/10.1111/j.1365-2222.2011.03779.x>.
 42. Lee SA, Noel S, Sadasivam M, Allaf ME, Pierorazio PM, Hamad ARA, Rabb H. Characterization of kidney CD45^{int}CD11b^{int}F4/80+MHCI+CX3CR1+Ly6C⁺ “intermediate mononuclear phagocytic cells.” *PLoS ONE*. 2018;13(6):e0198608. <https://doi.org/10.1371/journal.pone.0198608>.
 43. Lei F, Cui N, Zhou C, Chodosh J, Vavvas DG, Paschalis EI. CSF1R inhibition by a small-molecule inhibitor is not microglia specific; affecting hematopoiesis and the function of macrophages. *Proc Natl Acad Sci USA*. 2020. <https://doi.org/10.1073/pnas.1922788117>.
 44. Lei F, Cui N, Zhou C, Chodosh J, Vavvas DG, Paschalis EI. CSF1R inhibition by a small-molecule inhibitor is not microglia specific; affecting hematopoiesis and the function of macrophages. *Proc Natl Acad Sci USA*. 2020;117(38):23336–8. <https://doi.org/10.1073/pnas.1922788117>.
 45. Li X, Gao X, Zhang W, Liu M, Han Z, Li M, Lei P, Liu Q. Microglial replacement in the aged brain restricts neuroinflammation following intracerebral hemorrhage. *Cell Death Dis*. 2022;13(1):33. <https://doi.org/10.1038/s41419-021-04424-x>.
 46. Lu YC, Yeh WC, Ohashi PS. LPS/TLR4 signal transduction pathway. *Cytokine*. 2008;42(2):145–51. <https://doi.org/10.1016/j.cyto.2008.01.006>.
 47. Martina MN, Bandapalle S, Rabb H, Hamad AR. Isolation of double negative alpha T cells from the kidney. *J Vis Exp*. 2014; (87). <https://doi.org/10.3791/51192>.
 48. McKercher SR, Torbett BE, Anderson KL, Henkel GW, Vestal DJ, Baribault H, Klemsz M, Feeney AJ, Wu GE, Paige CJ, Maki RA. Targeted disruption of the PU.1 gene results in multiple hematopoietic abnormalities. *EMBO J*. 1996;15(20):5647–58.
 49. Merry TL, Brooks AES, Masson SW, Adams SE, Jaiswal JK, Jamieson SMF, Shepherd PR. The CSF1 receptor inhibitor pexidartinib (PLX3397) reduces tissue macrophage levels without affecting glucose homeostasis in mice. *Int J Obes (Lond)*. 2020;44(1):245–53. <https://doi.org/10.1038/s41366-019-0355-7>.
 50. Mirrione MM, Konomos DK, Gravanis I, Dewey SL, Aguzzi A, Heppner FL, Tsirka SE. Microglial ablation and lipopolysaccharide preconditioning affects pilocarpine-induced seizures in mice. *Neurobiol Dis*. 2010;39(1):85–97. <https://doi.org/10.1016/j.nbd.2010.04.001>.
 51. Moynagh PN. TLR signalling and activation of IRFs: revisiting old friends from the NF-kappaB pathway. *Trends Immunol*. 2005;26(9):469–76. <https://doi.org/10.1016/j.it.2005.06.009>.
 52. Mun SH, Park PSU, Park-Min KH. The M-CSF receptor in osteoclasts and beyond. *Exp Mol Med*. 2020;52(8):1239–54. <https://doi.org/10.1038/s12276-020-0484-z>.
 53. Nandi S, Gokhan S, Dai XM, Wei S, Enikolopov G, Lin H, Mehler MF, Stanley ER. The CSF-1 receptor ligands IL-34 and CSF-1 exhibit distinct developmental brain expression patterns and regulate neural progenitor cell maintenance and maturation. *Dev Biol*. 2012;367(2):100–13. <https://doi.org/10.1016/j.ydbio.2012.03.026>.
 54. Nelson LH, Lenz KM. Microglia depletion in early life programs persistent changes in social, mood-related, and locomotor behavior in male and female rats. *Behav Brain Res*. 2017;316:279–93. <https://doi.org/10.1016/j.bbr.2016.09.006>.
 55. Ngkelo A, Meja K, Yeaton M, Adcock I, Kirkham PA. LPS induced inflammatory responses in human peripheral blood mononuclear cells is mediated through NOX4 and Gialpha dependent PI-3kinase signalling. *J Inflamm (Lond)*. 2012;9(1):1. <https://doi.org/10.1186/1476-9255-9-1>.
 56. Nimmerjahn A, Kirchhoff F, Helmchen F. Resting microglial cells are highly dynamic surveillants of brain parenchyma in vivo. *Science*. 2005;308(5726):1314–8. <https://doi.org/10.1126/science.1110647>.
 57. Paolicelli RC, Bolasco G, Pagani F, Maggi L, Scianni M, Panzanelli P, Giustetto M, Ferreira TA, Guiducci E, Dumas L, Ragozzino D, Gross CT. Synaptic pruning by microglia is necessary for normal brain development. *Science*. 2011;333(6048):1456–8. <https://doi.org/10.1126/science.1202529>.
 58. Parkhurst CN, Yang G, Nanan I, Savas JN, Yates JR, Lafaille JJ, Hempstead BL, Littman DR, Gan W-B. Microglia promote learning-dependent synapse formation through brain-derived neurotrophic factor. *Cell*. 2013;155(7):1596–609. <https://doi.org/10.1016/j.cell.2013.11.030>.
 59. Rubino SJ, Mayo L, Wimmer I, Siedler V, Brunner F, Hametner S, Madi A, Lanser A, Moreira T, Donnelly D, Cox L, Rezende RM, Butovsky O, Lassmann H, Weiner HL. Acute microglia ablation induces neurodegeneration in the somatosensory system. *Nat Commun*. 2018;9(1):4578. <https://doi.org/10.1038/s41467-018-05929-4>.
 60. Scott EW, Simon MC, Anastasi J, Singh H. Requirement of transcription factor PU.1 in the development of multiple hematopoietic lineages. *Science*. 1994;265(5178):1573–7.
 61. Shi Y, Manis M, Long J, Wang K, Sullivan PM, Remolina Serrano J, Hoyle R, Holtzman DM. Microglia drive APOE-dependent neurodegeneration in a tauopathy mouse model. *J Exp Med*. 2019;216(11):2546–61. <https://doi.org/10.1084/jem.20190980>.
 62. Shibuya Y, Kumar KK, Mader MM, Yoo Y, Ayala LA, Zhou M, Mohr MA, Neumayer G, Kumar I, Yamamoto R, Marcoux P, Liou B, Bennett FC, Nakauchi H, Sun Y, Chen X, Heppner FL, Wyss-Coray T, Sudhof TC, Wernig M. Treatment of a genetic brain disease by CNS-wide microglia replacement. *Sci Transl Med*. 2022;14(636):eab9945. <https://doi.org/10.1126/scitranslmed.abl9945>.
 63. Sierra A, Encinas JM, Deudero JJ, Chancey JH, Enikolopov G, Overstreet-Wadiche LS, Tsirka SE, Maletic-Savatic M. Microglia shape adult

- hippocampal neurogenesis through apoptosis-coupled phagocytosis. *Cell Stem Cell*. 2010;7(4):483–95. <https://doi.org/10.1016/j.stem.2010.08.014>.
64. Skrzypczak-Wiercioch A, Salat K. Lipopolysaccharide-induced model of neuroinflammation: mechanisms of action, research application and future directions for its use. *Molecules*. 2022;27(17):5481. <https://doi.org/10.3390/molecules27175481>.
 65. Sweet MJ, Hume DA. Endotoxin signal transduction in macrophages. *J Leukoc Biol*. 1996;60(1):8–26. <https://doi.org/10.1002/jlb.60.1.8>.
 66. Szalay G, Martinecz B, Lenart N, Kornyei Z, Orsolits B, Judak L, Csaszar E, Fekete R, West BL, Katona G, Rozsa B, Denes A. Microglia protect against brain injury and their selective elimination dysregulates neuronal network activity after stroke. *Nat Commun*. 2016;7:11499. <https://doi.org/10.1038/ncomms11499>.
 67. Tap WD, Wainberg ZA, Anthony SP, Ibrahim PN, Zhang C, Healey JH, Chmielowski B, Staddon AP, Cohn AL, Shapiro GI, Keedy VL, Singh AS, Puzanov I, Kwak EL, Wagner AJ, Von Hoff DD, Weiss GJ, Ramanathan RK, Zhang J, Habets G, Zhang Y, Burton EA, Visor G, Sanftner L, Severson P, Nguyen H, Kim MJ, Marimuthu A, Tsang G, Shellooe R, Gee C, West BL, Hirth P, Nolop K, van de Rijn M, Hsu HH, Peterfy C, Lin PS, Tong-Starkens Bollag S, G. Structure-guided blockade of CSF1R kinase in tenosynovial giant-cell tumor. *N Engl J Med*. 2015;373(5):428–37. <https://doi.org/10.1056/NEJMoa1411366>.
 68. Tecklenborg J, Clayton D, Siebert S, Coley SM. The role of the immune system in kidney disease. *Clin Exp Immunol*. 2018;192(2):142–50. <https://doi.org/10.1111/cei.13119>.
 69. Torres L, Danver J, Ji K, Miyauchi JT, Chen D, Anderson ME, West BL, Robinson JK, Tsirka SE. Dynamic microglial modulation of spatial learning and social behavior. *Brain Behav Immun*. 2016;55:6–16. <https://doi.org/10.1016/j.bbi.2015.09.001>.
 70. Tremblay ME, Lowery RL, Majewska AK. Microglial interactions with synapses are modulated by visual experience. *PLoS Biol*. 2010;8(11):e1000527. <https://doi.org/10.1371/journal.pbio.1000527>.
 71. Vichaya EG, Malik S, Sominsky L, Ford BG, Spencer SJ, Dantzer R. Microglia depletion fails to abrogate inflammation-induced sickness in mice and rats. *J Neuroinflammation*. 2020;17(1):172. <https://doi.org/10.1186/s12974-020-01832-2>.
 72. Wake H, Moorhouse AJ, Jinno S, Kohsaka S, Nabekura J. Resting microglia directly monitor the functional state of synapses in vivo and determine the fate of ischemic terminals. *J Neurosci*. 2009;29(13):3974–80. <https://doi.org/10.1523/JNEUROSCI.4363-08.2009>.
 73. Wang Y, Szretter KJ, Vermi W, Gilfillan S, Rossini C, Cella M, Barrow AD, Diamond MS, Colonna M. IL-34 is a tissue-restricted ligand of CSF1R required for the development of Langerhans cells and microglia. *Nat Immunol*. 2012;13(8):753–60. <https://doi.org/10.1038/ni.2360>.
 74. Wang YR, Mao XF, Wu HY, Wang YX. Liposome-encapsulated clodronate specifically depletes spinal microglia and reduces initial neuropathic pain. *Biochem Biophys Res Commun*. 2018;499(3):499–505. <https://doi.org/10.1016/j.bbrc.2018.03.177>.
 75. Warden AS, Triplett TA, Lyu A, Grantham EK, Azzam MM, DaCosta A, Mason S, Blednov YA, Ehrlich LIR, Mayfield RD, Harris RA. Microglia depletion and alcohol: transcriptome and behavioral profiles. *Addict Biol*. 2021;26(2):e12889. <https://doi.org/10.1111/adb.12889>.
 76. Wegiel J, Wisniewski HM, Dziewiatkowski J, Tarnawski M, Kozielski R, Trenkner E, Wiktor-Jedrzejczak W. Reduced number and altered morphology of microglial cells in colony stimulating factor-1-deficient osteopetrotic op/op mice. *Brain Res*. 1998;804(1):135–9. [https://doi.org/10.1016/s0006-8993\(98\)00618-0](https://doi.org/10.1016/s0006-8993(98)00618-0).
 77. Wlodarczyk A, Holtman IR, Krueger M, Yogev N, Bruttger J, Khoroshii R, Benmamar-Badel A, de Boer-Bergsma JJ, Martin NA, Karram K, Kramer I, Boddeke EW, Waisman A, Eggen BJ, Owens T. A novel microglial subset plays a key role in myelinogenesis in developing brain. *EMBO J*. 2017;36(22):3292–308. <https://doi.org/10.15252/embj.201696056>.
 78. Wolf AA, Yanez A, Barman PK, Goodridge HS. The ontogeny of monocyte subsets. *Front Immunol*. 2019;10:1642. <https://doi.org/10.3389/fimmu.2019.01642>.
 79. Wu W, Li Y, Wei Y, Bosco DB, Xie M, Zhao MG, Richardson JR, Wu LJ. Microglial depletion aggravates the severity of acute and chronic seizures in mice. *Brain Behav Immun*. 2020;89:245–55. <https://doi.org/10.1016/j.bbi.2020.06.028>.
 80. Yan X, Anzai A, Katsumata Y, Matsuhashi T, Ito K, Endo J, Yamamoto T, Takeshima A, Shinmura K, Shen W, Fukuda K, Sano M. Temporal dynamics of cardiac immune cell accumulation following acute myocardial infarction. *J Mol Cell Cardiol*. 2013;62:24–35. <https://doi.org/10.1016/j.yjmcc.2013.04.023>.
 81. Zembower TR. Epidemiology of infections in cancer patients. *Cancer Treat Res*. 2014;161:43–89. https://doi.org/10.1007/978-3-319-04220-6_2.

Publisher's Note

Springer Nature remains neutral with regard to jurisdictional claims in published maps and institutional affiliations.

Ready to submit your research? Choose BMC and benefit from:

- fast, convenient online submission
- thorough peer review by experienced researchers in your field
- rapid publication on acceptance
- support for research data, including large and complex data types
- gold Open Access which fosters wider collaboration and increased citations
- maximum visibility for your research: over 100M website views per year

At BMC, research is always in progress.

Learn more biomedcentral.com/submissions

